

CFD Simulation and Validation of Flap Type Wave-Maker

Anant Lal, and M. Elangovan

Abstract—A general purpose viscous flow solver Ansys CFX was used to solve the unsteady three-dimensional (3D) Reynolds Averaged Navier-Stokes Equation (RANSE) for simulating a 3D numerical viscous wave tank. A flap-type wave generator was incorporated in the computational domain to generate the desired incident waves. Authors have made effort to study the physical behaviors of Flap type wave maker with governing parameters. Dependency of the water fill depth, Time period of oscillations and amplitude of oscillations of flap were studied. Effort has been made to establish relations between parameters. A validation study was also carried out against CFD methodology with wave maker theory. It has been observed that CFD results are in good agreement with theoretical results. Beaches of different slopes were introduced to damp the wave, so that it should not cause any reflection from boundary. As a conclusion this methodology can simulate the experimental wave-maker for regular wave generation for different wave length and amplitudes.

Keywords—CFD, RANSE, Flap type, wave-maker, VOF, seakeeping, numerical method.

NOMENCLATURE

Af = flap stroke length
 Aw = wave amplitude
 H = wave height
 hf = Height of stationary wall below flap
 hw = water height
 S = stroke length
 Tp = Time period
 θ = rotation angle of flap
 $Xdisp$ = displacement of flap at z
 Pi = point location for wave elevation

SUBSCRIPTS

f = flap
 w = wave
 p = period of flap movement

I. INTRODUCTION

STUDY of water wave is very important in the field of marine hydrodynamics to estimate the hydrodynamic forces, motion analysis and wave pattern. Experimental wave tank is one of the methods to find out some of the solutions

Anant Lal is with the Indian Register of Shipping, Mumbai 400072, India (phone: +91-22-30519603; fax: +91-22-25703611; e-mail: anant.lal@irclass.org).

M. Elangovan is with the Indian Register of Shipping, Mumbai 400072, India (phone: +91-22-30519521; fax: +91-22-25703611; e-mail: m.elangovan@irclass.org).

related to the seakeeping performance of a ship or offshore structure. The wave tank is usually characterized as long and narrow enclosures with a wave-maker at one end [1-3]. Moreover, a beach is installed at the end of the tank to damp the wave.

Now a day's efforts are being given to establish numerical technique to get the accurate prediction of experimental results. CFD method is an important tool which can substitute the experimental wave tank due to flexibility in modeling and simulations. Some researchers are working in the area to establish a Numerical Wave Tank (NWT), which can generate the desired wave [4-5]. With the availability of more computational resource, it is possible to solve Reynolds Averaged Navier-Stokes Equation (RANSE) which gives solution of real flow problems.

To simulate wave propagation in the numerical wave tank, the elevation of free surface has to be calculated for each time step. It can be calculated using an interface tracking method, where computational grid is adapted to the moving free surface boundary for each time step, or with an interface capturing method, solving an additional transport equation for the free surface. Interface capturing methods are performed on a time dependent computational grid. The present simulation uses interface capturing method using RANSE and the VOF method [6].

A numerical wave tank has been modeled whose dimension was taken as an experimental wave tank. Waves are generated using flap type wave-maker. A beach is introduced in the end of the tank to reduce the effect of reflected wave. Generated wave profile, wave height and wave length for different cases were studied depending on flap stroke length (Af), Time period (Tp), Fill height and other governing parameters. Accuracy of the computed results were verified against flap type wave-maker theory.

II. NUMERICAL METHOD

A. Problem Setup

Objective of the present paper is to establish the CFD modeling and simulation of regular wave for the analysis of ship or offshore structure. Flap type wave maker is selected to generate the wave in a wave tank using a beach to dampen the wave, so that there should not be any reflection of wave. Simulations have been made for the wave tank of nearly practical dimensions. Schematic diagram of the wave maker is shown in Fig. 1. Nomenclature used for the simulation is shown in Fig. 2.

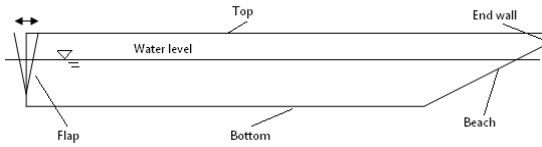


Fig. 1 2D schematic diagram for flap wave maker

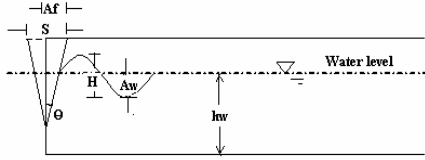


Fig. 2 Typical view of tank profile view and wave elevation

B. Computational Domain and Grid Generation

Modeling of geometry and meshing were done using ICEM CFD AI Environment. Dimensions of the computational domain and locations of the wave height predictions are given in Fig. 4 and Table I respectively. Structured grids were generated for all the cases (different beach slopes) using blocking arrangements. Finer mesh was adopted near the free surface level, to capture more accurate movement of free surface (Fig. 3).

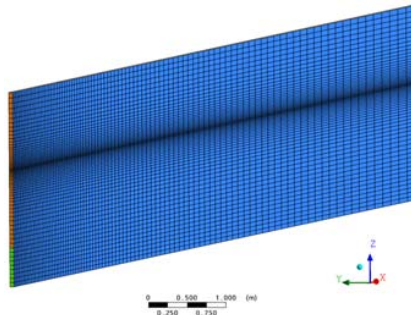


Fig. 3 Typical mesh for 2D wave maker (Refine mesh near the free surface)

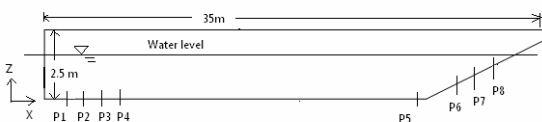


Fig. 4 Point locations for wave height prediction

TABLE I
LOCATIONS OF WAVE ELEVATION MEASUREMENT

Points	Location (x in m)
P1	1
P2	2
P3	3
P4	4
P5	28
P6	30.5
P7	32
P8	33.5

C. Numerical Simulations and Boundary Conditions

General purpose RANSE solver Ansys CFX, which is based on Finite Volume Method (FVM), was used for the present simulation. Multiphase simulations for free surface deformation were captured using Volume of Fraction (VOF) method. The governing equation for viscous flow includes continuity equation, momentum, volume fraction and turbulence model equations [8].

The governing equation for Mass and Momentum equation are:

$$\frac{d\rho}{dt} + \nabla \cdot \rho \mathbf{v} = 0 \quad (1)$$

$$\frac{d}{dt} \rho \mathbf{v} + \nabla \cdot \rho \mathbf{v} - \nabla p + \nabla \cdot \boldsymbol{\tau} = 0 \quad (2)$$

Where, \mathbf{v} is the velocity vector in the Cartesian co-ordinate system, p is the static pressure and $\boldsymbol{\tau}$ is the stress tensor, given by:

$$\boldsymbol{\tau} = \mu[(\nabla \mathbf{v} + \nabla \mathbf{v}^T) - 2/3(\nabla \cdot \mathbf{v})\mathbf{I}] \quad (3)$$

Where, μ is the molecular viscosity, \mathbf{I} is the unit tensor.

VOF Method

Volume Fraction of the q^{th} fluid, α_q the appropriate variable and properties are assigned to each cell within the domain. Tracking of the interfaces is done through the solution of continuity equation for the volume fraction of the phases. For the q^{th} phase

$$\frac{d}{dt} \alpha_q + \mathbf{v} \cdot \nabla \alpha_q = 0 \quad (4)$$

$$\sum_{q=1}^n \alpha_q = 1 \quad (5)$$

A single momentum equation is solved throughout the domain, and the resulting velocity field is shared among the phases. The momentum equation depends upon the Volume Fraction (VF) of all phases through the fluid properties, which is determined by the presence in each control volume,

$$\rho = \sum_{q=1}^n \alpha_q \cdot \rho_q \quad (6)$$

Duration of each transient simulation was fixed to 20s. Time step size of 0.02s was used, which was decided based on courant number criterion.

Boundary Conditions (BCs)

Bottom, beach, slope and end wall of the domain were given as wall with no slip with top as opening with pressure as atmospheric pressure. Motion of the flap (Fig. 5) was implement through mesh motion giving specified displacement using CFX Expression Language (CEL) [8].

See Eqn. (7)

$$X_{disp} = \{(z - hf)/(D - hf)\} * Af * \sin(\omega t) \quad (7)$$

where, X_{disp} is the displacement of flap at corresponding z location on the flap. Rotation angle of flap (Θ) and A_f is related as

$$\tan \theta = A_f / (D - hf) \quad (8)$$

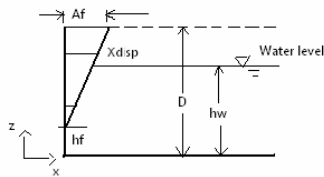


Fig. 5 Typical Flap movement mechanism

Initialisations

Global initial condition was set to velocity in all the direction as zero, static pressure as hydrostatic pressure with turbulent KE and eddy dissipation rate as automatic with value.

D. Grid Dependency Study

In numerical analysis, density of elements plays an important role. Therefore three cases have been taken with different mesh size, which is tabulated in Table II.

Table II shows three cases depending on size of grid used for grid dependency study. Fig. 6 shows the comparison of wave elevation at a location between different grid sizes.

TABLE II
TOTAL NO. ELEMENTS FOR DIFFERENT MESH TYPE

Cases:	Type:	No. of Elements:
Case1	Coarse	5,115
Case2	Normal	9,246
Case3	Fine	15,921

Predicted wave elevations at location P1 (Table I) for three different mesh sizes don't show very great change in result. Rest of the simulations was done using normal mesh size.

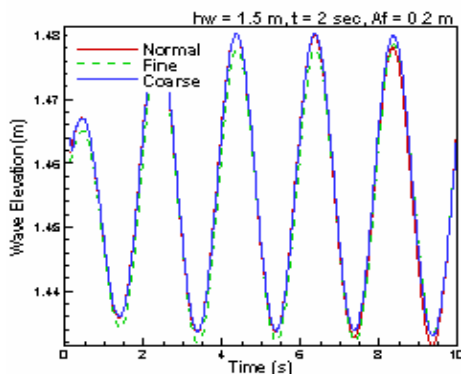


Fig. 6 Comparison of wave elevations at location P1 for different type of grid sizes

E. Turbulence Model Study

Fig. 7 shows the time history of wave elevation predicted at P1 (Table I) in the tank for different turbulence model as Laminar, K-ε and SST turbulence model. It is noted that the

difference is not remarkable in the results between different turbulence models.

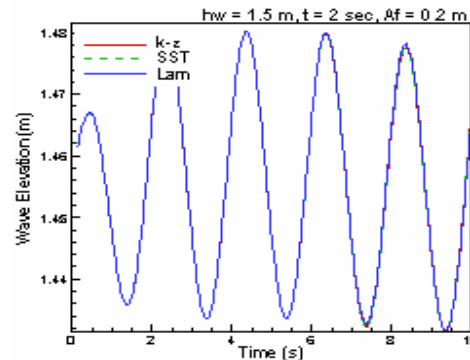


Fig. 7 Time history of wave elevation at location P1 for different turbulence model

III. RESULTS AND DISCUSSIONS

Aim of the paper is to generate wave numerically using CFD, from wave-maker so it can be used as a wave basin for a model analysis. Physical parameter of a wave in wave tank mainly depend on three factors namely water height, flap displacement and period of Stroke displacement. Authors have made the effort to establish the relation between flap stroke length (A_f), Time period (T_p), water height (hw) and also with angular displacement (Θ). Simulated cases for dependency study have been tabulated below in Table III.

TABLE III
TEST CASES

hw (m)	Tp (s)	Af (m)	Θ (°)	Θ/T_p (deg./s)
0.75	1.5	0.2	5	2.5 (0.04631 rad/s)
1.0	2	0.3	10	
1.25	3	0.4	15	
1.5	4	0.5	20	
1.6	5		25	

A. Validation of CFD Results with Wave-Maker Theory

To generate the wave by flap type wave maker, the relation between stroke length, water height and wave height is given [7] by

$$S = H \frac{\sinh khw + khw}{2(\cosh khw - 1)} \quad (8)$$

Where, S is the stroke length, H is the wave height, hw is water height. This has been derived from linear wave-maker theory. Here $S = 2A_f$ (Flap stroke length)

Predicted CFD results were compared with wave-maker theory (WMT) as shown in Fig. 8. A very good agreement between CFD and WMT results validates the methodology.

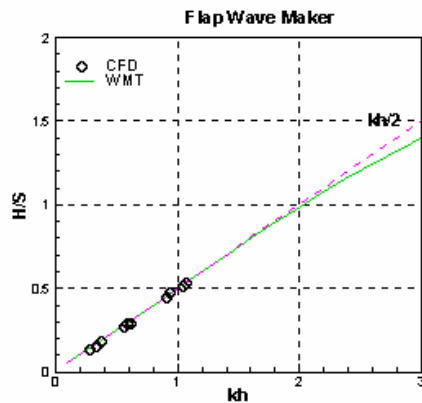


Fig. 8 Comparison of Computed results from CFD and wave-maker theory

B. Flap Stroke Length (Af) Dependency

Dependency of stroke length at constant water height (hw) and at a particular Time period (Tp) was studied. A typical result of time history of wave elevation at locations P1, P2 and P3 is shown in Fig. 9 ($hw=1.5m$, $Tp=2s$, $\theta=5.7^\circ$; $Af=0.2m$). Wave profile along the length of the tank is shown in Fig. 10. Fig. 11 shows computed time history of wave elevation at a location for different flap rotation angle.

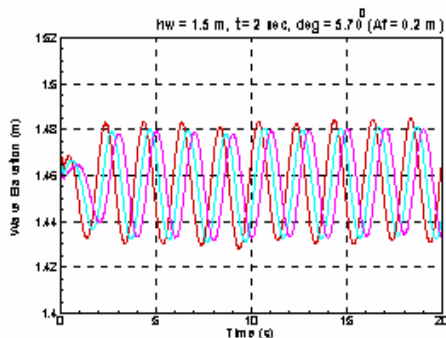


Fig. 9 Typical time history of wave elevation at locations P1, P2 and P3 for flap stroke length $Af=0.2m$

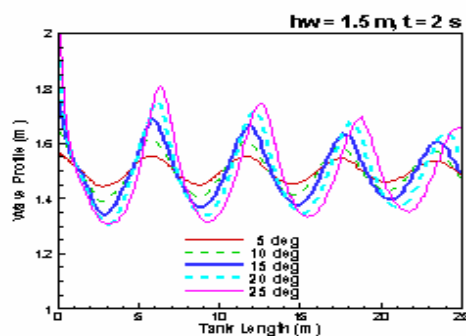


Fig. 10 Wave profile along the tank length for different angular displacement $\theta = 5^\circ, 10^\circ, 15^\circ, 20^\circ, 25^\circ$

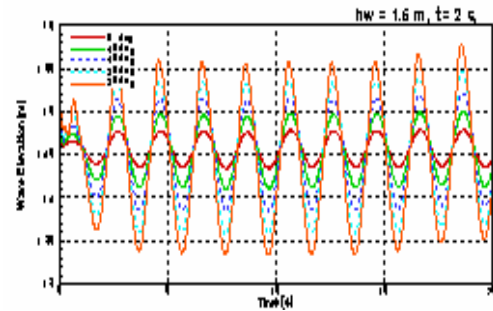


Fig. 11 Predicted wave elevation at location P2 in the tank for variation of $\theta = 5^\circ, 10^\circ, 15^\circ, 20^\circ, 25^\circ$

It has been observed that wave height and wavelength are directly proportional to stroke length (Figs. 12 & 13) i.e. increase in stroke length gives increase in wave height as well as wavelength. Similar type of result was also obtained for variation of flap angular displacement (θ), see Figs. 14 & 15.

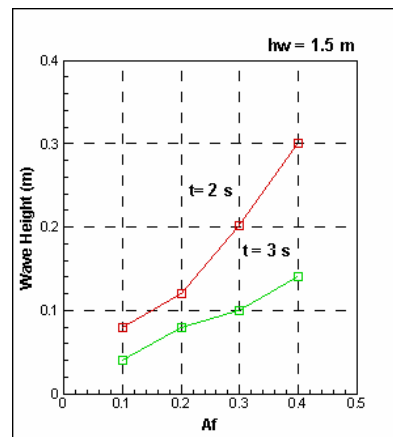


Fig. 12 Wave height vs. Flap stroke length

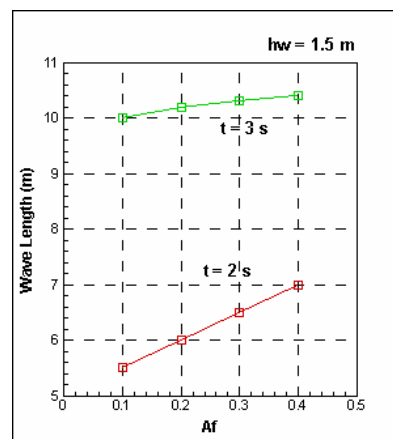


Fig. 13 Wavelength vs. Flap stroke length

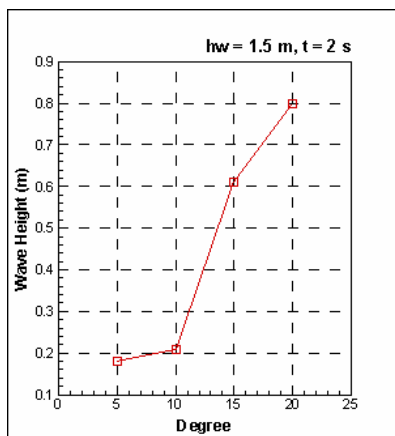


Fig. 14 Wave height vs. Flap angular displacement

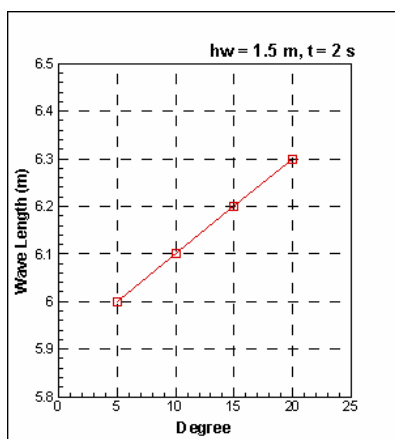


Fig. 15 Wavelength vs. Flap angular displacement

C. Time Period (T_p) Dependency

At constant flap stroke length (A_f or θ) and at constant water height (hw), dependency of the wave height elevation with different time period was simulated. Wave profile along the tank for different T_p is shown in Fig. 16. Wave height and wave length decreases with the increase in time period (T_p) at constant angular displacement.

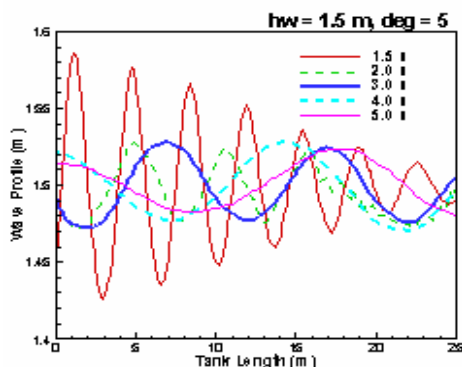
Fig. 16 Wave profile for different T_p

Fig. 17 shows the dependency of wave height at different time period of flap movement at constant angular displacement ($\theta = 5^\circ$). Period corresponding to 3s gives more wave height as compare to others periods, which gives the information that max. wave height is possible at a particular period by fixing the others parameters. We tried to simulate the same condition for 1s period, but the wave generation is not proper; this means that any choice of time period may not be able to form the wave. Wavelength increases as increase in time period, the trend is similar as previous results (Fig. 18).

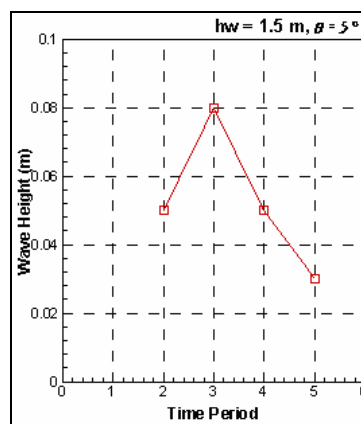


Fig. 17 Wave height vs. Time period

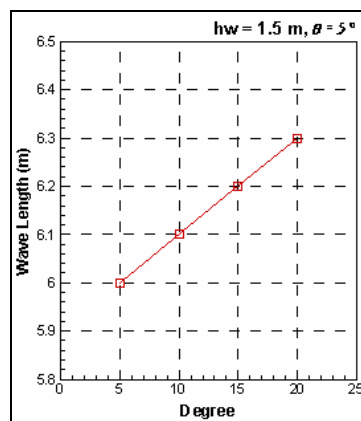


Fig. 18 Wavelength vs. Time period

D. Water Height(hw) Dependency

Effect of changing water height (hw) for particular flap stroke length (A_f or θ) and particular T_p were simulated. Results are plotted in Figs. 19 & 20 respectively. Wave height and wavelength both increases with increase in fill water height (hw). It has also been observed that generation of wave is not possible from lowering the water height (hw) from a limit.

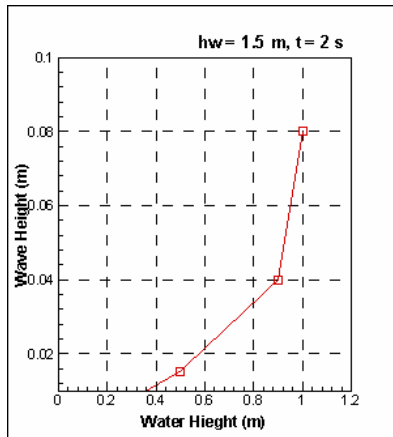


Fig. 19 Wave height vs. Water height

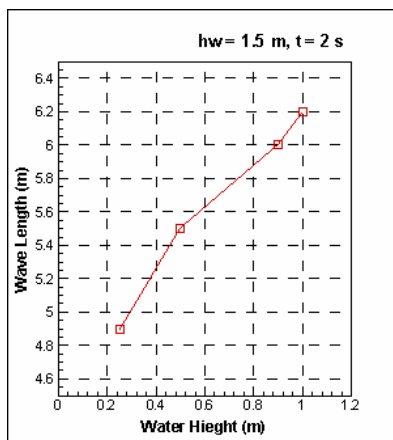
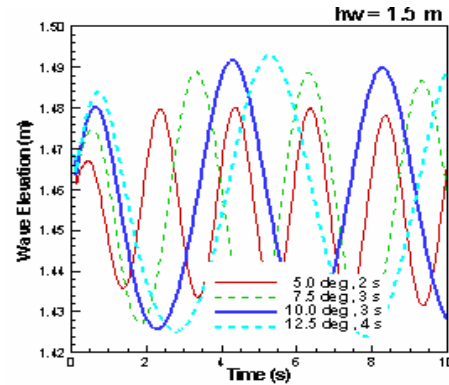
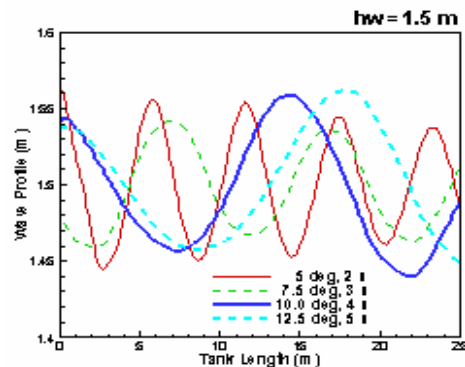
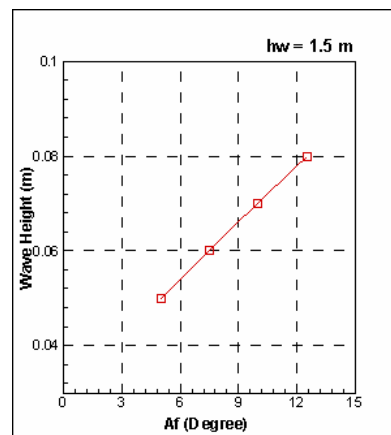


Fig. 20 Wavelength vs. Water height

E. Flap Movement at Constant (θ/T_p) Ratio

Since any combination of A_f and T_p doesn't produce the wave. So we tried to simulate some cases, by varying both θ and T_p but keeping (θ/T_p) ratio as fixed, Ratio was taken as the case which gives better wave generation depending upon the nature of wave height and wavelength. Simulations have been carried out for different $T_p = 2s, 3s, 4s$ and $5s$ at constant ratio of $\theta = 5^\circ$ and $T_p = 2s$, which gives the ratio of 2.5 deg/s (0.0436 rad/s). Fig. 21 shows the time history of wave elevation for different values of T_p at a particular location in the tank. So it is observed that by generating a particular wave, variation can be studied more easily by fixing ratio as constant. Wave profile along the tank is shown in Fig. 22. Wave height and wavelength at different T_p are shown in Figs. 23 & 24 respectively.

Fig. 21 Time history of wave elevation for different cases (at constant θ/T_p ratio)Fig. 22 wave profile for different T_p , along the tank (at constant θ/T_p ratio)Fig. 23 Wave height vs. Time period (At constant θ/T_p ratio)

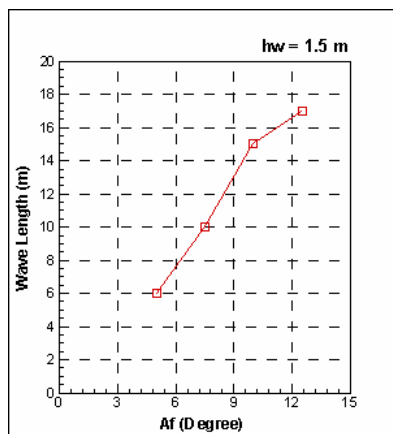


Fig. 24 Wavelength vs. Time period
(At constant θ/T_p ratio)

F. Damping of Wave at Different Beach Sloping

It is necessary to introduce a beach of certain slope so that not to cause any disturbance in wave elevation in the area of interest. By introducing a suitable beach slope damping can be done easily. Fig. 25 shows the time history of wave elevation at locations P1 and P6. It is found that wave elevation is not getting changed at initial location of the tank after a long time of simulation which makes the effectiveness of the beach.

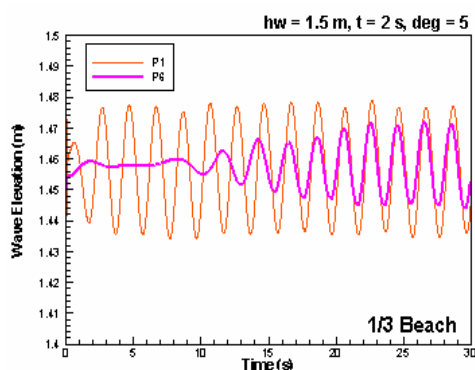


Fig. 25 Wave elevation at P1 and P6 for 1:3 slope beach

Effort has been made to study the damping nature of wave by introducing different beach slopes as 1:3, 1:4.5 and 1:6. Damping of the wave elevation is more in case of 1:3 slope ratios as shown in Fig. 26.

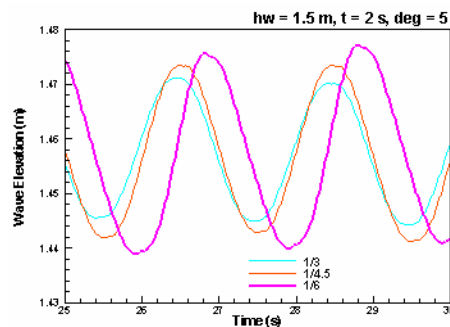


Fig. 26 Wave elevation for different beach slope

IV. CONCLUSION

Effort has been made to establish the guidelines for the simulation of flap type wave-maker using CFD. Characteristics of the wave were studied by varying the governing parameters. Computed results are in good agreement with wave-maker theory. Results can be used for establishing an experimental wave-maker with knowing the limitations about generation of the wave. Finally it is concluded that CFD simulation can effectively replace wave-maker for the generation of regular wave.

ACKNOWLEDGEMENT

Authors would like to thank to all in R&D division who are directly or indirectly involved to carry out the work for the publication of the paper.

REFERENCES

- [1] Joe Longo et. al. "IIHR Towing Tank wave maker", Iowa Institute of Hydraulic Research, Iowa city, IA 52242.
- [2] Tommi Mikkola, "Simulation of Plunger type wave maker", Journal of Structural Mechanics.
- [3] J.R.M. Taylor, M.Rea, D.J. Rogers, "The Edinburgh Curved Tank", Internet source.
- [4] C. M. Dong and C. J. Hunang, "2- dimensional wave tank in viscous fluid", Proceedings of 11th International offshore and polar Engineering conference, Stavanger, Norway, June 17-22, 2001.
- [5] J. C. Park et. al., "Reproduction of fully Nonlinear Multidirectional waves by a 3D viscous Numerical wave Tank" Proceedings of 11th International offshore and polar Engineering conference, Stavanger, Norway, June 17-22, 2001.
- [6] Hirt, C.W. and Nichols, B.D., "Volume of fluid (VOF) method for the dynamics of free boundaries", Journal of Computational physics 39, 201, 1981.
- [7] Robert G. Dean and Robert A. Dalrymple "Water Wave mechanics, for Engineers and Scientists".
- [8] Ansys CFX Tutorial 11.0

Anant Lal is graduated in Civil Engineering from NIT Trichy, India in 2005. He is presently working in Hydrodynamics Group as Assistant Surveyor in R&D. He has more than three years experience in the area of application of CFD technology in marine and its related fields.

M. Elangovan is doing his PhD course in Hiroshima University in the field of Naval Architecture. He has served for National Ship Design and Research Center, India for more than five years and carried out many research projects for marine industry. He has published technical papers in international journals and international conferences. He has got overseas experiences on design of ship and consultancy projects. Presently, working as a surveyor in Hydrodynamics groups and doing research on sea-keeping by CFD and Boundary Element Method.